



Original Research Article

Bovine adipose tissue-derived mesenchymal stem cells self-assemble with testicular cells and integrates and modifies the structure of a testicular organoids

Jahaira Cortez ^{a, b}, Cristian G. Torres ^a, Víctor H. Parraguez ^a, Mónica De los Reyes ^a, Oscar A. Peralta ^{a, *}

^a Faculty of Veterinary and Animal Sciences, University of Chile, Santa Rosa 11735, Santiago 8820808 Chile

^b Doctorate Program of Forestry, Agriculture, and Veterinary Sciences (DCSAV), University of Chile, Santa Rosa 11315, Santiago 8820808 Chile

ARTICLE INFO

Keywords:

Mesenchymal stem cells
3D-culture
Testicular organoid
Germ cell transdifferentiation

ABSTRACT

Mesenchymal stem cells (MSC) display self-renewal and mesodermal differentiation potentials. These characteristics make them potentially useful for *in vitro* derivation of gametes, which may constitute experimental therapies for human and animal reproduction. Organoids provide a spatial support and may simulate a cellular niche for *in vitro* studies. In this study, we aimed at evaluating the potential integration of fetal bovine MSCs derived from adipose tissue (AT-MSCs) in testicular organoids (TOs), their spatial distribution with testicular cells during TO formation and their potential for germ cell differentiation. TOs were developed using Leydig, Sertoli, and peritubular myoid cells that were previously isolated from bovine testes ($n = 6$). Thereafter, TOs were characterized using immunofluorescence and Q-PCR to detect testicular cell-specific markers. AT-MSCs were labeled with PKH26 and then cultured with testicular cells at a concentration of 1×10^6 cells per well in Ultra Low Attachment U-shape bottom (ULA) plates. TOs formed by testicular cells and AT-MSCs (TOs + AT-MSCs) maintained a rounded structure throughout the 28-day culture period and did not show significant differences in their diameters. Conversely, control TOs exhibited a compact structure until day 7 of culture, while on day 28 they displayed cellular extensions around their structure. Control TOs had greater ($P < 0.05$) diameters compared to TOs + AT-MSCs. AT-MSCs induced an increase in proportion of Leydig and peritubular myoid cells in TOs + AT-MSCs; however, did not induce changes in the overall gene expression of testicular cell-specific markers. STAR immunolabelling detected Leydig cells that migrated from the central area to the periphery and formed branches in control TOs. However, in TOs + AT-MSCs, Leydig cells formed a compact peripheral layer. Sertoli cells immunodetected using WT1 marker were observed within the central area forming clusters of cells in TOs + AT-MSCs. The expression of COL1A associated to peritubular myoids cells was restricted to the central region in TOs + AT-MSCs. Thus, during a 28-day culture period, fetal bovine AT-MSCs integrated and modified the structure of the TOs, by restricting formation of branches, limiting the overall increase in diameters and increasing the proportions of Leydig and peritubular myoid cells. AT-MSCs also induced a reorganization of testicular cells, changing their distribution and particularly the location of Leydig cells.

1. Introduction

Mesenchymal stem cells (MSCs) are adult progenitor cells characterized by their multipotent differentiation potential toward various mesodermal lineages, including osteogenic, adipogenic, and chondrogenic [1]. In addition to their differentiation capacity, MSCs possess self-renewal potential, which allow them to maintain a reserve of undiffer-

entiated and multipotent cells in tissues for regenerative function [2,3]. MSCs can be isolated from several tissues, including among others, adipose, umbilical cord, synovial membrane, dental pulp, amniotic and chorionic membrane [4–6]. Their unique properties and broad tissue distribution make MSCs a promising tool for various therapeutic approaches and research efforts in the field of regenerative biology and medicine [7].

* Corresponding author. Escuela de Medicina Veterinaria, Facultad de Agronomía e Ingeniería Forestal, Facultad de Ciencias Biológicas y Facultad de Medicina, Pontificia Universidad Católica de Chile, Santiago, Chile, Vicuña Mackenna 4860, Macul, Santiago 7820436 Chile.

E-mail address: oscar.peralta@uc.cl (O.A. Peralta).

<https://doi.org/10.1016/j.theriogenology.2023.12.013>

Received 12 September 2023; Received in revised form 21 November 2023; Accepted 8 December 2023

0093-691/© 20XX

The potential therapeutic applications of MSCs are mainly associated to their advantages for isolation, differentiation and trophic potential associated to regenerative capacity. Unlike other types of stem cells, MSCs can be obtained at various stages of development and in adulthood, making them an abundant autologous or allogenic source for cell therapy. These properties make MSCs an useful tool in diverse areas of regenerative medicine, while also an alternative to overcome ethical limitations associated with the use of embryonic stem cells (ESCs). Numerous preclinical and clinical trials have confirmed the efficacy of MSCs in various diseases. In reproductive medicine, MSCs have been experimentally used for the treatment of reproductive disorders both in females and males [8–10]. It has been described that MSCs from various sources have the ability to restore ovarian function and promote follicular development, producing factors such as IGF, VEGF and others, which can restore tissue function and reduce apoptosis in pathologies such as premature ovarian failure (POF) and primary ovarian insufficiency (POI) [2,10]. In males, MSC therapy has been used in the treatments of azoospermia and oligozoospermia [8]. Additionally, it has been documented that exosomes released by MSCs possess the capability to support the spermatogenic process within the testes of animal models afflicted with infertility [11]. In accordance with these and other studies, MSCs sourced from various tissues have exhibited the capacity to differentiate into germ cell-like cells, as evidenced by the expression of germ cell markers [12–14]. In light of these findings, MSCs hold promise as a viable therapeutic avenue for addressing issues of infertility.

The testicular niche can be defined as the anatomical space where spermatogonial stem cells (SSC) differentiate and develop under control of signals, from surrounding cells and the support of extracellular matrix (ECM). In testis, the cellular components of the niche of spermatogonia would include Sertoli, Leydig, peritubular, endothelial and nerve cells [15,16]. By comprehensively studying and elucidating the complex microenvironment in which germ cells reside, researchers can gain insights into the crucial factors and signaling pathways involved in germ cell development, maturation, and function. This knowledge can lead to the development of targeted interventions and therapies to address infertility issues, such as optimizing *in vitro* culture conditions, enhancing germ cell survival and differentiation, and identifying novel approaches for germ cell transplantation or regenerative therapies. Ultimately, a profound understanding of the germ cell niche holds the potential to revolutionize infertility treatments and improve reproductive outcomes.

In recent years, the use of 3D cultures, such as organoids, has become important *in vitro* tools for cell modeling purposes. One of the objectives of the organoid culture is to recreate cellular niche or environment, providing *in vitro* cultured cells with conditions similar to those of a tissue [17]. Essentially, 3D cultures allow for functional differentiation, which is not achievable in 2D cultures, as the latter do not provide the necessary conditions for the cellular organization and interaction observed *in vivo* [18]. Regardless of the type of organoid, the basic components include: 1) basement membrane extract or hydrogel, such as Matrigel; 2) tissue-specific stem or progenitor cells; and 3) culture medium containing growth factors that mimic *in vivo* signaling [19–21].

Despite the growing interest in organoid systems over the past decade, testicular organoids (TOs) have only recently started to garner attention. One of the first reports on TOs were generated from primary adult and pubertal human testicular cells, which were capable to auto-assemble without a testicular scaffold [22]. Also in 2017, TOs from testicular rat cells and human immortalized Leydig and Sertoli cells were reported [23,24]. These TOs were able to secrete inhibin B, testosterone and cytokines. Sertoli cells in TOs also gave rise to tight junction proteins and appeared to support germ cell development. Since then, TOs have been generated in other species such as pigs, primate and mice [16,25,26]. Recently, our group isolated Leydig, Sertoli and peritubular

myoids cells to generate the first reported bovine TOs by using ULA plate culture system [27]. These bovine TOs displayed specific locations for Leydig, Sertoli and peritubular myoid cells, and were able to produce testosterone and increase its concentrations after 27 days of culture [27].

Despite the numerous therapeutic properties of MSCs, *in vitro* models based on MSCs still have limited applications, possibly, in part, due to a lack of knowledge regarding their mechanisms of action. Currently, there is a pressing need for novel biotechnological interventions to address infertility. The development of TOs presents promising potential in this context. The therapeutic function of MSCs is grounded on their capacity to differentiate into cells in need of replacement, alongside their immunomodulatory and paracrine activities, as well as their antioxidative effect contributing to tissue healing. The utilization of MSCs in conjunction with TOs emerges as an intriguing strategy that holds promise in addressing this issue, which has not been evaluated before. The co-culture of adipose tissue MSCs (AT-MSCs) with TOs presents a unique opportunity to study the effect of MSC on testicular cell populations. AT-MSCs have been reported to offer certain advantages compared to BM-MSCs (bone marrow-derived mesenchymal stem cells), such as their easier isolation, faster *in vitro* growth, and even a higher quantity within AT when compared to BM [42,52,63–65]. In this study we aimed at evaluating the potential integration of fetal bovine AT-MSCs in TOs (TOs + AT-MSCs) and their spatial distribution with testicular cells during TOs formation. Furthermore, we developed and used TOs to recreate the testicular niche under *in vitro* conditions and to evaluate the potential of AT-MSCs for differentiation into germ cells.

2. Materials and methods

2.1. Ethics

All experimental procedures have been approved and were performed in accordance with the guidelines and regulations of the Bioethical Committees of the Faculty of Veterinary and Animal Sciences at the University of Chile (Certificate N° 19266-VET-UCH) and the Pontifical Catholic University of Chile (Certificate N° 230315003).

2.2. Isolation of bovine AT-MSCs

Bovine fetal MSCs were obtained from AT isolated from the abdominal omentum. Under aseptic condition, approximately 10 g of AT were excised from the omentum of each fetus and were transferred to a tube containing 20 mL of PBS (pH 7.4; Hyclone Laboratories, Utah, USA), supplemented with 100 µg/mL streptomycin, 100 U/mL penicillin, and 0.25 mg/mL amphotericin B. Subsequently, the AT was incubated in an enzymatic solution containing 0.5 % type 1 collagenase (Sigma-Aldrich, MO, USA) diluted in balanced Hanks' saline solution (HBSS) (1 mL/g of AT) for manual disaggregation. The tissue was then incubated with agitation for 45 min at 37 °C. The disaggregated tissue was filtered through 40 µm pores and then centrifuged at 400 g for 5 min. The cell pellet was resuspended in expansion medium (DMEM supplemented with 10 % fetal bovine serum (FBS), 100 µg/mL streptomycin, 100 U/mL penicillin, and 0.25 mg/mL amphotericin B) and transferred to T75 culture bottles (Falcon, New Jersey, USA) at 38 °C in a humid atmosphere with 5 % CO₂. The non-adherent cells were removed by changing the culture medium after 2 days. The cells were expanded until the 3rd passage, reaching 90 % confluence. Subsequently, AT-MSCs were cryopreserved in expansion medium with 10 % DMSO in liquid nitrogen until the beginning of the experiments.

2.3. AT-MSC membrane labelling with PKH26

AT-MSCs were collected as previously described and labeled with PKH26 dye following the manufacturer's instructions (Sigma-Aldrich,

MO, USA) to track their localization in the TOs. Briefly, the cells were resuspended and then centrifuged ($400 \times g$) for 5 min to obtain a loose pellet. Subsequently, the supernatant was removed, and 1 mL of diluent C was added to the cell pellet, which was gently pipetted to ensure complete dispersion. A dye solution was prepared by adding 4 μ L of PKH26 to 1 mL of Diluent C. Quickly, 1 mL of cell suspension was added to 1 mL of dye solution and mixed immediately. The stained cells were incubated for 1–5 min, followed by the addition of 2 mL of serum and an additional incubation for 1 min. Cells were then centrifuged at $400 \times g$ for 10 min at 20–25 °C, and the supernatant was carefully removed. Subsequently, they were resuspended in 10 mL of culture medium, transferred to a new tube, and centrifuged two more times at $400 \times g$ for 5 min each with culture medium to ensure the removal of unbound dye. Finally, cells were resuspended in standard culture medium.

2.4. Bovine testis collection and preparation

A total of 6 bovine puberal testis (7–11 month) were used to obtain testicular cells. Testis were initially washed with calcium-magnesium free HBSS (Hyclone Laboratories, Utah, USA) supplemented with 100 μ g/mL streptomycin and 100 U/mL penicillin (HBSS P/E). Subsequently, the tunica albuginea was removed, and the parenchyma was carefully dissected. Approximately 15 g of testicular tissue were cut into fragments. The tissue fragments were then suspended in HBSS P/E and allowed to settle by gravity, after which the supernatant containing germ cells was discarded to separate the testicular cells from the extracellular matrix.

2.4.1. Isolation of bovine sertoli and myoids peritubular cells

Testicular cell isolation from bovine testis was performed following a previously established protocol [27,28]. The testicular tissue was further incubated in a beaker containing HBSS P/E at a ratio of 3:1 (tissue volume to HBSS P/E volume) and agitated at 37 °C for 20 min. Following this, the supernatant was discarded, and an enzymatic solution composed of HBSS P/S, 2.5 % trypsin, 1 % type IV collagenase, and 1 mg of DNase, was added for an additional 25-min incubation period. The resulting cell suspension was then centrifuged at 200 g for 5 min, and the supernatant was discarded. The cell pellet was resuspended in DMEM-F12 medium supplemented with 100 U/mL penicillin and 100 μ g/mL streptomycin at a 10:1 vol ratio (DMEM to tissue). The cell suspension was allowed to settle by gravity for 30 min at room temperature, and the supernatant containing interstitial cells was collected for further isolation of Leydig cells. Meanwhile, the remaining tubular fragments, after sedimentation, were resuspended in DPBS containing 1 M glycine and 2 mM EDTA (pH 7.4) for 10 min to eliminate peritubular myoid cells. The suspension was subjected to gravity sedimentation twice, and the supernatant containing peritubular myoid cells was collected. These cells were subsequently centrifuged and cultured in MEM supplemented with 10 % FBS, 100 U/mL penicillin, 100 μ g/mL streptomycin, and 100 μ g/mL amphotericin B. The pellet obtained after centrifugation, containing Sertoli cells, was seeded in DMEM-F12 medium supplemented with 10 % FBS, 100 U/mL penicillin, 100 μ g/mL streptomycin, and 100 μ g/mL amphotericin B.

2.4.2. Purification of bovine leydig cells on discontinuous percoll gradient

The fraction enriched in Leydig cells and interstitial cells was subjected to gravity sedimentation for a duration of 15 min. Subsequently, Leydig cells and interstitial cells were recovered from the supernatant through centrifugation, employing a 5-min centrifugation at 200g. The resulting pellet was resuspended in culture medium and subjected to a discontinuous 5-layer Percoll gradient, comprising concentrations of 21, 26, 34, 60 and 100 % in PBS. After a 30-min centrifugation at 1500g, the cell bands between 26 and 34 %, as well as between 34 and 60 %, were collected separately. These collected cell bands were diluted with 2 vol of DMEM:F12 containing penicillin-streptomycin (P/

S), followed by a 10-min centrifugation at 200g. Subsequently, the cells were plated and cultured in DMEM:F12 with P/S and supplemented with 10 % fetal bovine serum (FBS). The culture medium was replaced every 2–3 days.

2.5. Three-dimensional co-culture of AT-MSCs and bovine testicular cells

AT-MSCs were trypsinized and labeled with PKH26 dye for tracking purposes during TO formation. AT-MSCs and testicular cells were co-suspended at a total concentration of 1×10^6 cells (1:1 concentration; 5×10^5 pool of testicular cells and 5×10^5 of AT-MSCs) per well in 100 μ L of standard culture medium in each of a 96-well Ultra-Low Attachment (ULA) U-shape bottom plate (Corning, NY, USA). The standard culture medium consisted of DMEM-F12 supplemented with 10 % fetal bovine serum (FBS) (Gibco, Grand Island, USA), 100 U/mL penicillin, 100 μ g/mL streptomycin, and 100 μ g/mL amphotericin B. After 7 days of culture, the cellular aggregates were incubated with 40 μ L of Matrigel® (Corning, NY, USA) for 10–20 min at 38 °C to facilitate solidification. Subsequently, control TOs (TOs without AT-MSCs) and TOs + AT-MSCs (TOs with AT-MSCs) were transferred to 6 cm diameter ULA plates in standard culture medium. The cultures were maintained at 36 °C under a humid atmosphere with 5 % CO₂ for an additional 21 days (total of 28 days). Culture medium was changed every two days. Three replicates were performed for each experiment. The cellular aggregates were evaluated using phase-contrast microscopy on days 0, 16, and 28 of culture. In addition, samples were collected on days 0, 16, and 28 to assess the expression of germ cell differentiation markers through immunofluorescence and Q-PCR analysis (Tables 1 and 2).

2.6. Quantitative-PCR analysis of testicular cell-specific markers in bovine TOs

The quantification of mRNA levels for the endogenous genes GAPDH and ACTIN, as well as of testicular cell markers α SMA, WT1, and STAR, and germ cell marker DAZL was performed using quantita-

Table 1

Primary and secondary antibodies used for AT-MSCs and testicular cells immunodetection.

Antibody	Target cell	P/N	Cat.	Dilution
Anti-CD73	Mesenquimal	Abcam	Ab133582	1:50
Anti-COL1A	Peritubular	Santa Cruz	sc-293,182	1:50
Anti-STAR ^a	Leydig	Abcam	ab96637	1:100
Anti-WT1 ^b	Sertoli	Abcam	ab89901	1:100
Goat anti-rabbit	Secondary	Abcam	ab97050	1:100

^a Wilm's Tumor 1.

^b Steroidogenic acute regulatory.

Table 2

Primer sequence used in QPCR analysis.

Gene	Nucleotide Sequence (5'-3')	Access Number
β -ACTINA	Forward CGCACCCTGGCATTGTGCAT	NM_173979.3
	Reverse TCCAAGCGCAGCTAGCAGAG	
α SMA ^a	Forward CAGCCGAGAACTTCAGGGAC	NM_001034502.1
	Reverse GGTGATGATGCCGTGCTCTA	
STAR ^b	Forward GACACGGTCATCACTCACGA	NM_174189.3
	Reverse TACGCTCACAAAGTCTCGGG	
WT1 ^c	Forward ACAGATGCACAGCGGAAGC	XM_015470745.2
	Reverse GGTGGTCGGAACGGGAGAA	
DAZL	Forward TCCAAGTTCACCAGTTCAGG	NM_001081725.1
	Reverse CGTCTGTATGCTCTGTCCAC	

^a Wilm's Tumor 1.

^b Steroidogenic acute regulatory.

^c Actin alpha 2, smooth muscle (α SMA).

tive real-time PCR (Q-PCR) (Table 2). Total RNA was extracted from the TOs using the GeneJet RNA purification kit (Thermo Fisher Scientific, MA, USA) following the manufacturer's instructions. Total mRNA was quantified using a Qubit 3.0 Fluorometer (Thermo Fisher, CA, USA). Genomic DNA was removed using a DNase I kit (Thermo Scientific, MA, USA). cDNA synthesis and amplification were performed using the Affinity Script qPCR cDNA Synthesis Kit (Agilent Technologies, CA, USA) and a TC1000-G thermocycler (SciLogex, CT, USA). The Q-PCR reaction utilized the Brilliant SYBR Green qPCR Master Mix (Agilent Technologies, CA, USA) and an Eco Real-Time PCR System (Illumina, CA, USA). cDNA amplification was carried out for 40 cycles, and the relative expression analysis was performed using the $\Delta\Delta C_t$ method.

2.7. Testicular organoid whole-mounting staining

The cellular distribution of Leydig cells, Sertoli cells, peritubular myoid cells, and AT-MSCs in TOs was analyzed using confocal immunofluorescence following a previously established protocol [62]. Briefly, TOs were fixed overnight in 4 % paraformaldehyde at 4 °C. Subsequently, antigen retrieval was performed by incubating the samples in a 10 mM sodium citrate aqueous solution containing 0.05 % Tween-20 (Merck, Frankfurt, Germany) at pH 6 for 15 min at 95 °C. After cooling down for 15–30 min, the samples were washed three times with PBS (phosphate-buffered saline) containing 0.1 % Tween-20. Permeabilization of the samples was carried out using Triton X-100 (Merck, Frankfurt, Germany) in 1X PBS for 2 h at room temperature. To block non-specific binding, the samples were incubated with 2 % bovine serum albumin (BSA) in PBS for 1 h at room temperature. Immunodetection of the target proteins was performed by incubating the samples with primary antibodies diluted in 2 % BSA (Table 1) for 4 days at 4 °C. Following primary antibody incubation, the samples were washed three times with 0.1 % Tween in PBS. Subsequently, the samples were incubated with secondary antibodies diluted in 2 % BSA for 2 days at 4 °C. Finally, the samples were counterstained with Pure Blu DAPI Nuclear Staining Dye (BioRad Hercules, CA, USA) to visualize the cell nuclei.

2.8. Digital image acquisition and processing

Digital images were acquired using a contrast phase microscope connected to a digital camera (Motic, China). Confocal images of TOs

were taken with a Zeiss LSM 700 confocal microscope (Carl Zeiss, Oberkochen, Germany) and digital 3D images were analyzed with ImageJ software (National Institute of Health, USA, v1.47). The diameter determination of TOs and TOs + AT-MSCs included both branched and unbranched areas.

2.9. Statistical analysis

Statistical analyses were performed on relative gene expression, diameters and testicular cell percentages on TOs and TOs + AT-MSCs using the Info Stat software (Cordova, Argentina). Each experimental setup was repeated at least three times. The means values for each replicate were analyzed by two-way ANOVA. Gene expression values, diameters and testicular cell percentages of control TOs and TOs + AT-MSCs between days of culture were analyzed using Tukey's multiple comparison test ($P < 0.05$).

3. Results

3.1. AT-MSCs used in TOs formation previously displayed a homogeneous and specific marker profile

AT-MSCs were isolated by adhesion to plastic culture dishes and were labeled with PKH26 probe for tracking in the TOs (Fig. 1A). The percentages of AT-MSCs present in the cultures were determined by immunodetection of the CD73 marker using flow cytometry. It was found that 91.9 ± 0.6 % of cells were positive for CD73 (Fig. 1B). Testicular cells were isolated from bovine testes using a protocol previously reported by our group [27]. Sertoli cells, Leydig cells and peritubular myoid cells were subsequently used to form bovine TOs (Fig. 1C).

3.2. AT-MSCs co-cultivated with testicular cells generated and modified TOs

AT-MSCs and testicular cells were cultured in ULA plates to form cell aggregates (Fig. 2A). Subsequently, these aggregates were collected and transferred to Matrigel and maintained in orbital shaking culture. TOs were examined at days 1, 3, 7, 14 and 28 after the initiation of culture. Compact and tight TOs were generated at day 1 in both experimental groups. TOs + AT-MSCs were uniform in shape during the en-

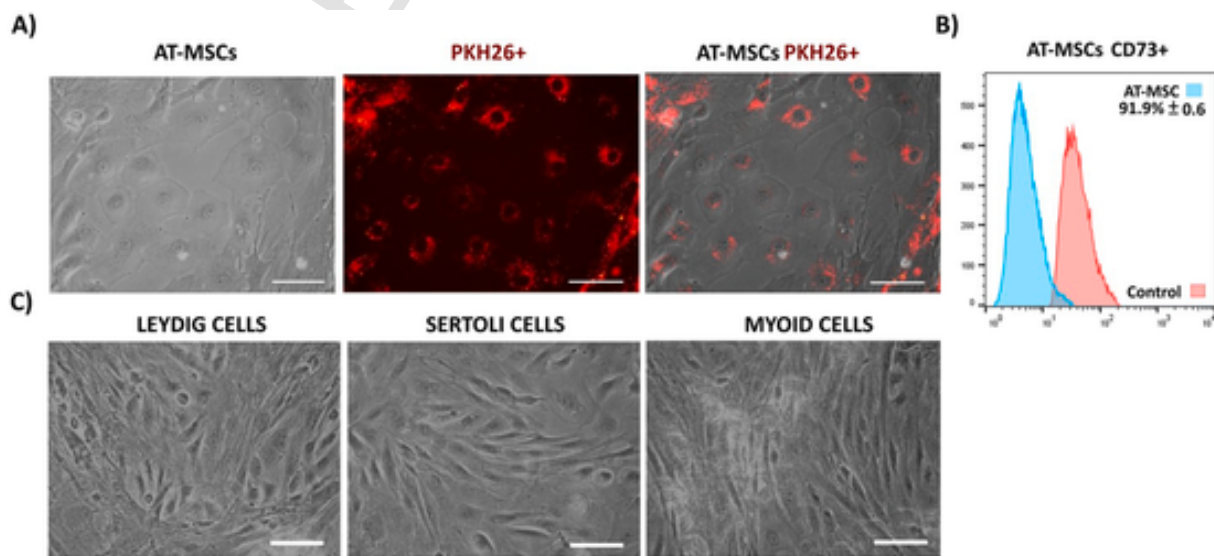


Fig. 1. Microphotograph of fetal bovine AT-MSCs labeled with PKH26 for tracking in TOs. (A) Monolayer culture of AT-MSCs after cryopreservation, thawing, and cultivation. PKH26-labeled bovine AT-MSCs visualized by epifluorescence microscopy. (B) Representative histogram of CD73-positive AT-MSCs used in the experiments and reported as means \pm ED. (C) Phase contrast micrograph of Leydig, Sertoli, and peritubular myoid cells isolated from testes. Testicular cells were cultured in monolayer and maintained up to the 5th or 6th passage. $n = 3$. Scale bar: 100 μ m.

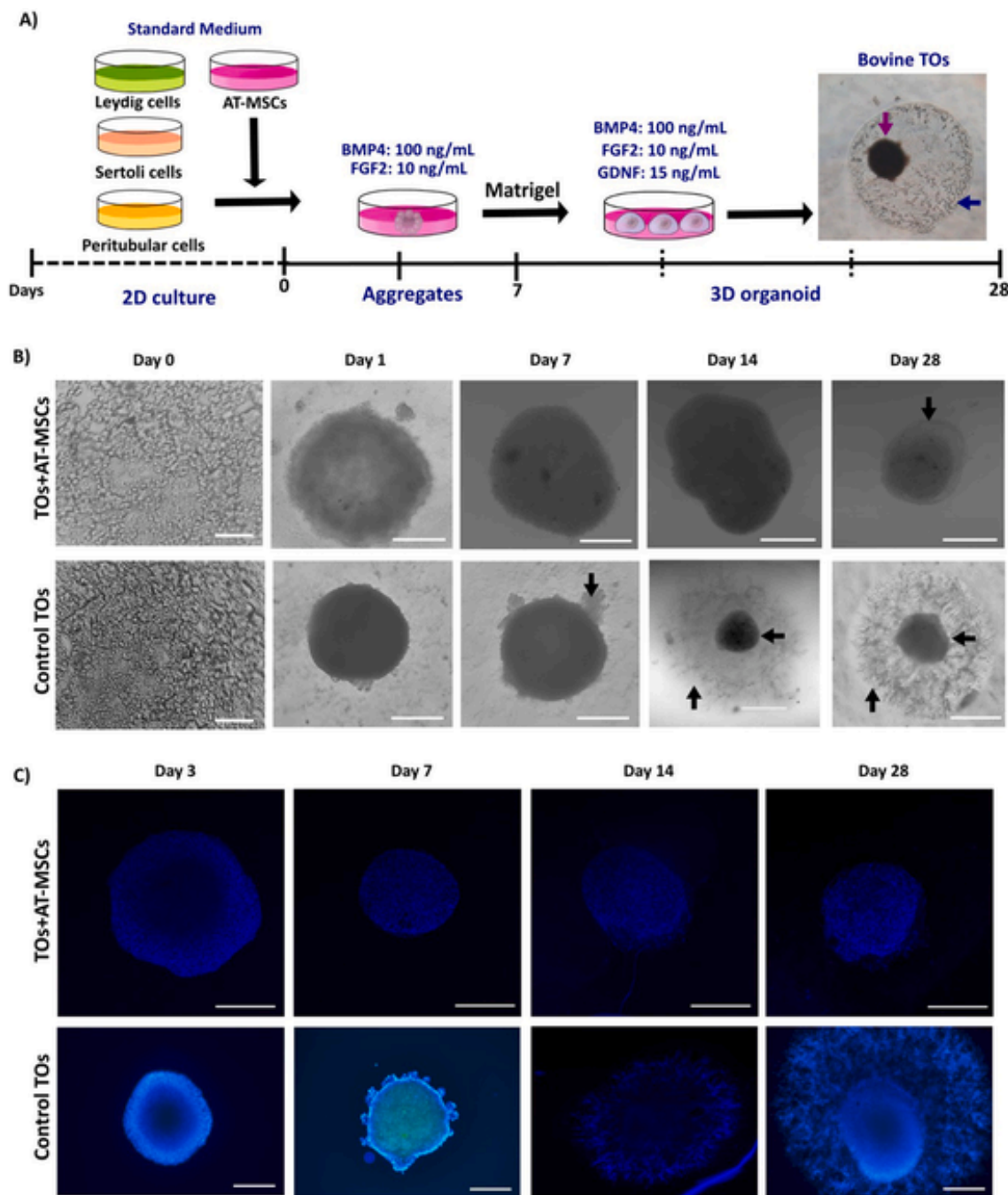


Fig. 2. Generation and morphological evaluation of bovine TOs derived from primary bovine testicular cells. (A) Schematic diagram for bovine TOs and TOs + AT-MSCs production (Blue arrow: Matrigel dome; purple arrow: TO). (B) Bright-field images of morphological changes and differences in cellular reorganization in TOs and TOs + AT-MSCs. Arrows indicate the outer layer in TOs + AT-MSCs and the presence of branches in control TOs, respectively. (C) Epifluorescence images of TOs + AT-MSCs and TOs stained with Dapi. (Scale bar = 100 μ m). Days 1, 7, 9, and 28 (Scale bar = 500 μ m). (For interpretation of the references to colour in this figure legend, the reader is referred to the Web version of this article.)

tire experiment, while control TOs became irregular with formations of branches since day 7 (Fig. 2B). Dapi cell-staining in TOs + AT-MSCs and control TOs at days 3, 7, 14 and 28 allowed to observe that AT-MSCs and testicular cells were mixed and packed together and self-assembled into forming TOs (Fig. 2C). Dapi staining allowed to identify numerous cell nuclei in control TO branches. The size of TOs + AT-MSCs fluctuated between 604 and 864 and the mean diameters were 808 μ m \pm 37.2 on day 3, 654 μ m \pm 25.4 on day 7, 647 μ m \pm 16.3 on day 14 and 596 μ m \pm 86.2 on day 28, with no significant differences between days (Fig. 3A). In the TOs + AT-MSCs, a layer of spherical-

shaped cells was observed surrounding the central area on day 28 of culture. The diameter of control TOs fluctuated between 555.15 and 1272.88 μ m and the mean diameter were 578 μ m \pm 12.7 at day 3, 794 μ m \pm 27.6 at day 7, 1096 μ m \pm 38.3 at day 14 and 1245 μ m \pm 14.2 at day 28. Diameters of control TOs included branched and unbranched areas and the average diameters were higher ($P < 0.05$) compared to TOs + AT-MSCs during the 28 days of culture (Fig. 3B).

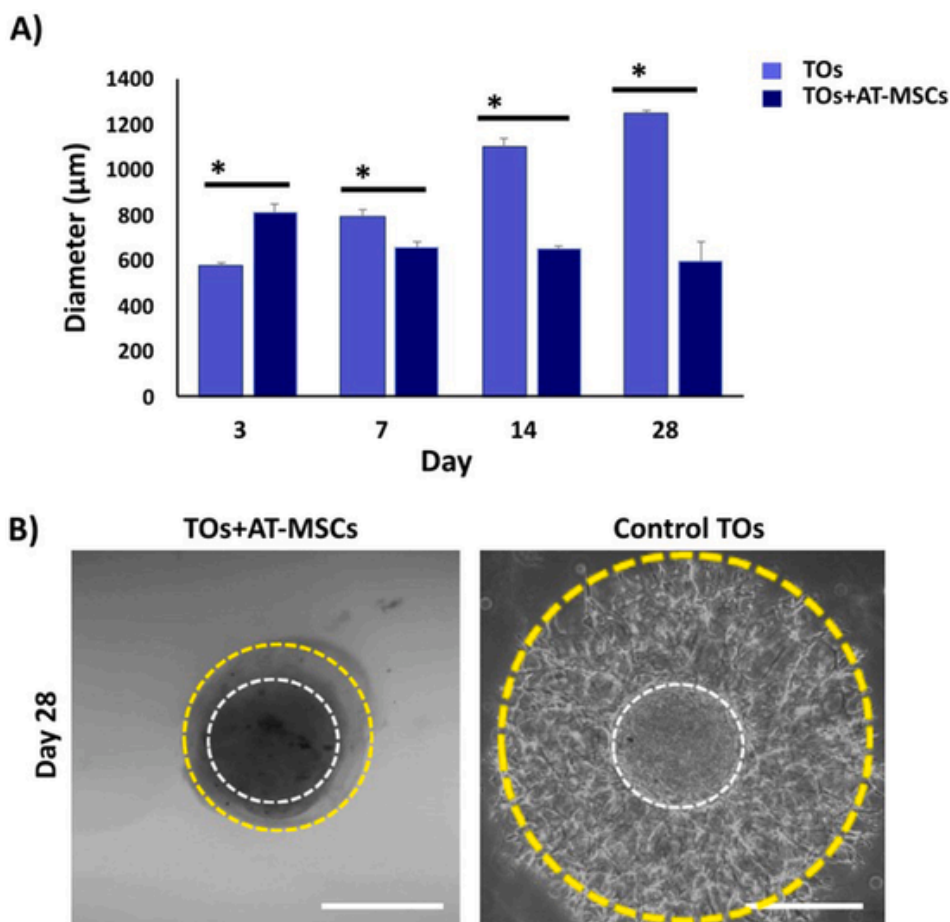


Fig. 3. Diameters and morphological comparison between bovine TOs and TOs + AT-MSCs. (A) TOs had a larger diameter ($P < 0.05$) compared to TOs + AT-MSCs co-cultures. (B) Phase contrast microphotograph of TOs and TOs + AT-MSCs on day 28 of culture, showing the presence of extensions in TOs and an outer layer of cells in TOs + AT-MSCs. $n = 3$. Superscript (*) indicates significant ($P < 0.05$) difference between TOs and TOs + AT-MSCs at each day of culture. Scale bar: 500 μm .

3.3. AT-MSCs induced an increased in percentages of leydig and peritubular myoid cells; however, did not exert changes in the overall gene expression of testicular cell-specific markers in TOs

The percentage of STAR-positive cells in control TOs decreased ($P < 0.05$) on days 14 and 28 ($61\% \pm 2.0$ and $34\% \pm 5.2$, respectively) compared to days 3 and 7 ($74\% \pm 23.1$ and $58\% \pm 22$, respectively) (Fig. 4A). Similarly, in TOs + AT-MSCs, the proportions of Leydig cells decreased ($P < 0.05$) from $76\% \pm 22.9$ (day 3) and $52\% \pm 38.1$ (day 7) to $60\% \pm 2.0$ (day 14) and $58\% \pm 7.9$ (day 28); however, at day 28 proportions of Leydig cells were higher ($P < 0.05$) in TOs + AT-MSCs compared to TOs. The percentage of WT1-positive cells in TOs increased ($P < 0.05$) from days 3 ($39\% \pm 9$) and 7 ($56\% \pm 3$) to day 28 ($59\% \pm 3.7$). In contrast, in TOs + AT-MSCs, cells positive for WT1 decreased from day 3 ($72\% \pm 12.0$) to days 14 and 28 ($54\% \pm 3.5$ and $52\% \pm 9$, respectively). Thus, on day 28, proportion of cells positive for WT1 were lower ($P < 0.05$) in TOs + AT-MSCs compared to TOs. Percentages of COL1A-positive cells in control TOs decreased ($P < 0.05$) from $44\% \pm 10$ (day 3) and $38\% \pm 10$ (day 7) to $35\% \pm 5.9$ (day 14) and $19\% \pm 2.1$ (day 28). Similarly, in TOs + AT-MSCs, cells positive for WT1 decreased ($P < 0.05$) from $45\% \pm 9.9$ (day 3) to $35\% \pm 5.9$ (day 14) and $44\% \pm 2.4$ (day 28). At day 28, proportion of COL1A-positive cells were higher ($P < 0.05$) in TOs + AT-MSCs compared to TOs. Levels of gene expression of selected specific-markers for Leydig, Sertoli, peritubular myoids and germ cells (STAR, WT1, α -SMA and DAZL) were analyzed in TOs and TOs + AT-MSCs throughout culture period. Levels of mRNA of STAR

(Leydig cells), WT1 (Sertoli cells), and α SMA (peritubular myoid cells) in TOs and TOs + AT-MSCs were similar ($P > 0.05$) during all days evaluated (Fig. 4B). Gene expression of DAZL was not detected neither in TOs nor in TOs + AT-MSCs.

3.4. AT-MSCs changed the distributions of somatic testicular cells in TOs

To investigate the spatial distribution of AT-MSCs and their association with testicular cells, PKH26-positive AT-MSCs were co-cultivated and co-localized with immunofluorescence associated to STAR (Leydig cells), WT1 (Sertoli cells) and COL1A (Peritubular myoid cells) in TOs-AT-MSCs during culture. At day 3, PKH26-positive AT-MSCs were located at the center of TOs + AT-MSCs, whereas Leydig cells were visualized in the peripheral areas (Fig. 5A and B). At day 7, AT-MSCs and Leydig cells displayed mixed locations in the whole TOs + AT-MSCs. From day 14–28, AT-MSCs were located at the center of TOs + AT-MSCs, whereas Leydig cells formed a delimited layer in the periphery. Leydig cells were located in the whole section, conforming the branches in control TOs. From days 3–28, Sertoli cells and PKH26-positive AT-MSCs were mainly detected in the central area of TO + AT-MSC, revealing some cell compartmentalization (Fig. 6A and B). In control TOs, Sertoli cells were mainly located in the central region. From days 3–28, peritubular myoid cells were located in the central area of TOs + AT-MSCs TOs (Fig. 7A and B). Similarly, AT-MSCs labeled with PKH26 were observed in the central region of TOs + AT-MSCs. Higher magnification allowed to detect a mixed location of peritubular myoid cells and AT-MSCs in the center of TOs + AT-MSCs.

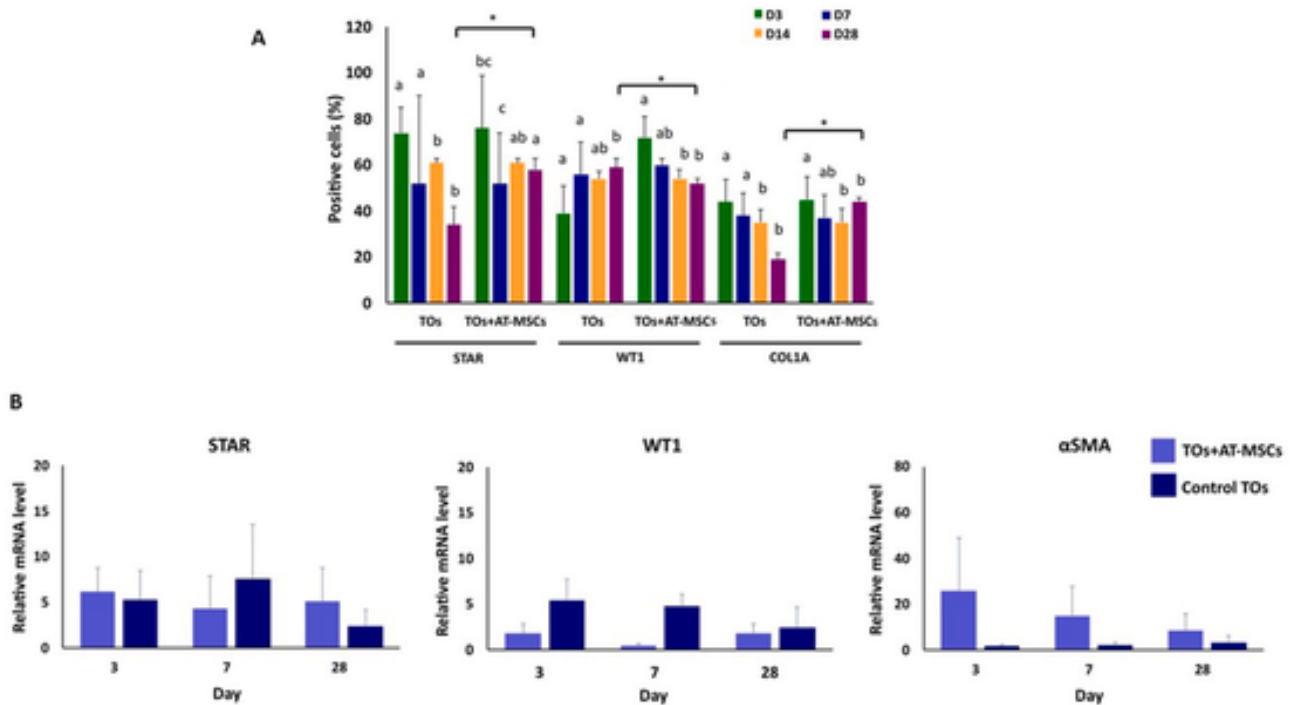


Fig. 4. Proportions of testicular cell types at days of culture and relative mRNA expression of testicular cell specific markers in TO and TOs + AT-MSCs. (A) Proportions of cells positive for STAR and COL1A were increased ($P < 0.05$); whereas percentages of cells positive for WT1 were decreased ($P < 0.05$) in TOs + AT-MSCs compared to TOs. (B) The mRNA levels of STAR (Leydig cells), WT1 (Sertoli cells), and α SMA (peritubular myoid cells) were not significantly different between TOs + AT-MSCs and control TOs at days 3, 7, and 28 of culture. ($n = 3$). Superscript (a,b,c) indicates significant ($P < 0.05$) difference for testicular cell proportion between days of culture for TOs or TOs + AT-MSCs and (*) indicates significant ($P < 0.05$) difference for testicular cell proportion between TOs and TOs + AT-MSCs at day 28 of culture.

3.5. Schematic representation of AT-MSCs and testicular cells in TOs revealed their cell-specific location and migration

The immunofluorescent labeling of testicular cells before formation of TOs proved to be a valuable technique for investigating the cellular organization within TOs. By employing confocal microscopy, we were able to precisely determine cell-specific spatial distribution and with this information we proposed a schematic representative model of TOs and TOs + AT-MSCs (Fig. 8). The observations from the projections of TOs + AT-MSCs and control TOs revealed that AT-MSCs within the TOs + AT-MSCs structure impacts the arrangement of Leydig cells. In the presence of AT-MSCs, Leydig cells do not locate in branching structures; instead, they assemble into a distinct layer surrounding the central region of the TOs. Sertoli cells and peritubular myoid cells were predominantly located in the central area of TOs, regardless of the presence of AT-MSCs. This schematic representation contributes to a deeper understanding of how AT-MSCs influence the formation of the TO structure.

4. Discussion

Organoids provide a means to replicate physiological and pathological processes under *in vitro* conditions, faithfully recreating cell integration, migration and cell-to-cell and cell-to-matrix interactions [20,29,30]. In this respect, TOs represent useful models for studying testicular physiology and germ cell biology. Processes and methodologies employed for production of TOs are highly diverse, ranging from variations in the numbers of testicular cells used to difference in culture methods applied [23,25,31]. Organoids derived from dissociated testicular cells can be cultured employing different techniques, including matrix-based or self-support methodologies, 3D printing and hanging-drop. Every methodology exhibits its distinct array of advantages and

drawbacks, as documented in the scientific literature [15,16,24,31,59,61]. One of the most commonly techniques used in organoid production is ECM scaffold method, due to its consistency for generating similar organoids. A disadvantage associated with this technique is the reproducible generation of natural or synthetic ECM that accurately mirrors the composition of ECM existing in the tissue [23,27,53,59]. Spinning bioreactor method enable the simultaneous production of a substantial quantity of 3D cultures, albeit with the drawback of yielding organoids of heterogeneous shapes. Despite being one of the most prevalent methods for organoid formation, its utilization has been limited to the context of TO development [60]. The hanging drop method is an air-liquid interface technique that relies on the accumulation of cells at the liquid-air interface, which does not require ECM for the straightforward and consistent formation of TOs [16,24]. Some disadvantages of this method include the inability to use liquid drops larger than 50 μ L and the difficulty of changing cell culture medium without the potential impact to the organoid [61]. The use of low-adherence cell culture plates is a simple and cost-effective method with a high throughput capability [26,27]. Nonetheless, it may not consistently yield organoids from certain cell types [61].

As part of this study, testicular cells were isolated from bull testis and subsequently co-cultured with fetal bovine AT-MSCs to evaluate the potential integration of these cells in TOs and their spatial distribution with testicular cells during TO formation. Furthermore, we developed and used TOs to recreate the testicular niche under *in vitro* conditions and to evaluate the potential differentiation of AT-MSCs into germ cells.

According to previous studies, the formation time of TOs varies between 2 and 9 days depending on the culture method and the number of cells used [24,31,32]. In TOs models, dissociated cells are initially distributed uniformly throughout the Matrigel, which extends the formation time. By using ULA plates at the beginning of the culture, the disso-

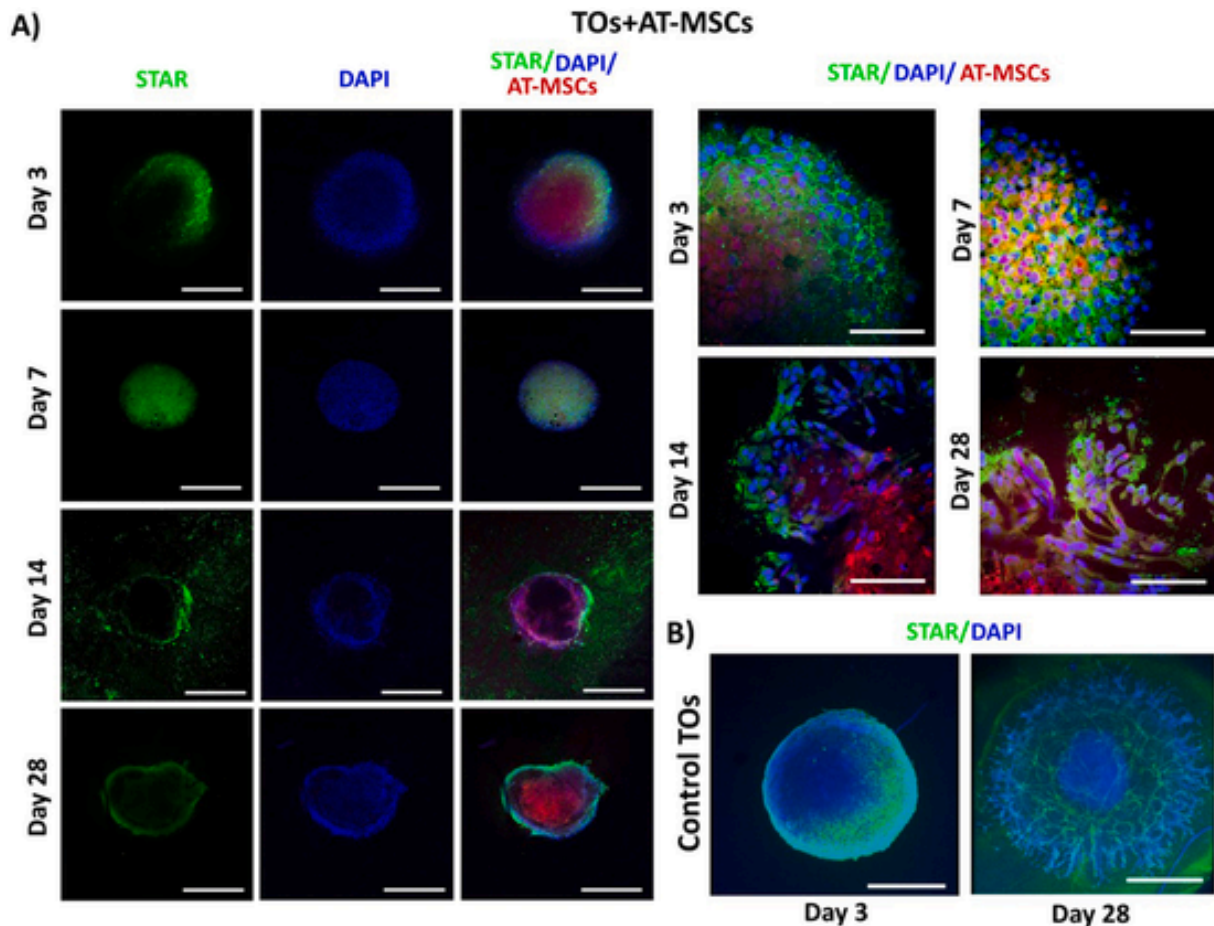


Fig. 5. Colocalization of Leydig cells and AT-MSCs in bovine TOs using confocal microscopy. (A) Immunolocalization of STAR in TOs during 28 days of culture. STAR-positive cells were distributed in the periphery of TOs + AT-MSCs and formed a defined peripheral layer from days 14–28. AT-MSCs (PKH26 red) were located in the central zone of TOs + AT-MSCs. (B) STAR expression in control TOs at days 3 and 28 of culture. Cell nuclei stained with DAPI. $n = 3$. Scale bars = 500 μm . (For interpretation of the references to colour in this figure legend, the reader is referred to the Web version of this article.)

ciated cells confluence in the U-shape dish bottom and interacts within each other more rapidly, facilitating the formation of a functional and representative *in vitro* model. In this study, the formation time for both TOs + AT-MSCs and control TOs was 24 h, indicating that the induction of proximity resulted in increased efficiency for TO production. The diameters of TOs have not always been reported, however some studies mentioned diameters between 100 and 600 μm , which represents a smaller range compared to diameters obtained in our study [17,24,32]. A previously reported protocol used in this study for generation of bovine TOs, was used for individual isolation of Leydig, Sertoli, and peritubular myoid cells and co-culture of these cells with AT-MSCs for TO formation [27]. This protocol also included culture of dissociated cells in ULA plates, which promoted cellular aggregation, maximizing cell-cell contact and facilitating formation of 3D structures [33]. In the present study, the newly formed bovine TOs were capable of maintaining somatic cell types including Sertoli, Leydig, peritubular myoid cells and to preserve AT-MSCs throughout the 28-Day culture period.

Only a few studies have integrated MSCs into organoids thus far and there is no report of co-culturing fetal bovine AT-MSCs with bovine testicular cells during formation of TOs [3,34]. Until now, utilization of MSCs in 3D co-cultures has demonstrated promising outcomes in various organoid models. For instance, studies involving pulmonary epithelial cell organoids have reported an enhanced formation efficiency and increased size when MSCs were incorporated into cultures [3,34]. A feature observed in our study was the distinct variation in diameter between TOs + AT-MSCs and control TOs. Specifically, when testicular

cells and AT-MSCs were co-cultured, TOs + AT-MSCs displayed a constant diameter that resulted to be smaller compared to control TOs. Moreover, TOs + AT-MSCs adopted a more compact morphology characterized by the absence of branches. Notably, a discernible layer of cells was also observed in the periphery of TOs + AT-MSCs. Some studies declared that MSCs have the capability to remodel the extracellular matrix (ECM), promoting tissue organization and structural integrity [35]. This has been observed in organoids and spheroids derived from cardiac, hepatic, and neural cells co-cultivated with MSCs [35,36]. Overall, our data indicate that AT-MSCs induced remodeling of the structure of the TOs, restricting formation of branches and limiting the overall increase in diameters during culture period.

PKH26-labeled AT-MSC in TOs + AT-MSCs were observed during the whole culture period, displaying a central and common location with Sertoli and peritubular myoid cells. One of the characteristics attributed to MSCs in 3D cultures is their ability to regulate cell migration. Previous investigations have revealed that MSCs effectively limit cell motility in 3D environments [37]. Another noteworthy attribute is that MSCs exert a protective effect by producing angiogenic factors and anti-apoptotic molecules, thereby modulating adaptive signaling pathways in neighboring cells [36,38]. Furthermore, MSC have been shown to influence cellular differentiation and proliferation, driving the development of functional and mature cell types within the organoid structures [39]. This characteristic may explain the observed absence of branching in TOs, suggesting that integration of AT-MSC influences the structural organization of the organoid. Moreover, given the changes in TOs morphology and considering that 3D structures, including

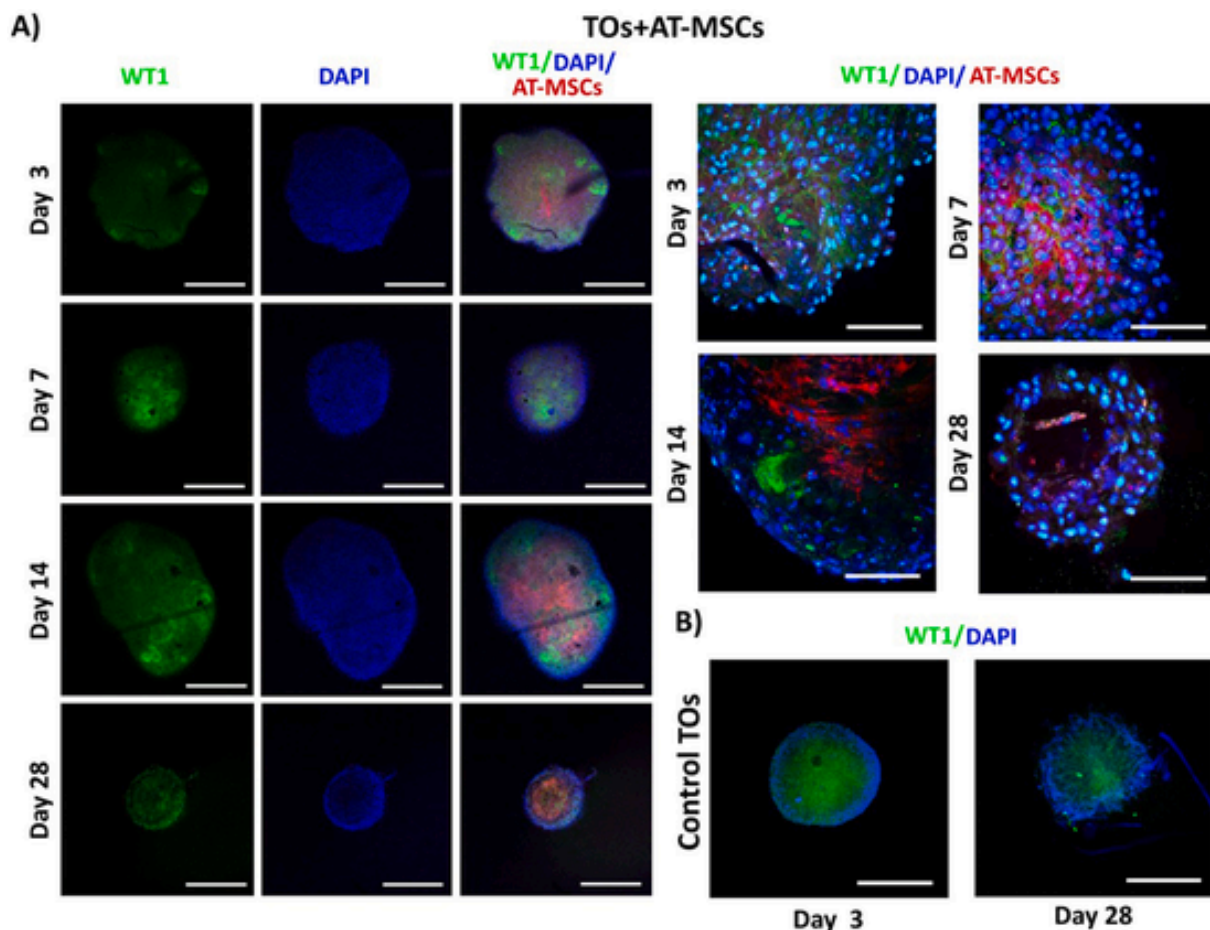


Fig. 6. Colocalization of Sertoli cells and AT-MSCs in bovine TOs using confocal microscopy. (A) WT1-positive cells in TOs + AT-MSCs were observed forming clusters of cells between days 3 and 14 of culture. By day 28, cells were distributed throughout the TOs. (B) WT1 expression in control bovine TOs at day 3 and 28 of culture. Cell nuclei were stained blue with DAPI. $n = 3$. Scale bars = 500 μm . (For interpretation of the references to colour in this figure legend, the reader is referred to the Web version of this article.)

organoids, can create a hypoxic central microenvironment [36], we can speculate that the presence of AT-MSCs in the central region could mitigate hypoxia-induced apoptosis, improving viability and adaptation under hypoxic conditions in TOs.

Cultures of isolated Leydig, Sertoli and peritubular myoid cells have been widely used in a variety of studies in cattle [40–42]. However, their isolation and culturing for the purpose of forming TOs had not been described in cattle. Leydig cells are responsible for testosterone production, which is an essential hormone that regulates spermatogenesis and the development of male sexual characteristics. Additionally, Leydig cells provide support for the structure of the seminiferous tubules and enable its contraction in the testis [43]. In the present study, Leydig cells isolated from bovine testes were identified in TOs based on the expression of the marker STAR, which corresponds to a transporter protein involved in cholesterol transfer during testosterone synthesis [44,45]. The location of STAR expression suggests that in control TOs, Leydig cells migrated from the central area to the peripheral branches; however, presence of AT-MSCs prevented this migration and determined formation of a compact structure in TOs + AT-MSCs. In testis, Sertoli cells are in direct contact with germ cells and are responsible for promoting germ cell progression towards spermatozoa. We identified bovine Sertoli cells using the WT1 marker, which plays a crucial role in the differentiation of somatic cells during gonadal development and maintains its expression in adult Sertoli cells [46,47]. In TOs + AT-MSCs, Sertoli cells were observed within the central area, revealing some compartmentalization in relation to AT-MSCs. This com-

partmentalization may also be associated with reduction in Sertoli cell proportion in TOs + AT-MSCs. It has been previously reported that Sertoli cells promote proliferation of MSCs via upregulation of genes involved in the regulation of the cell cycle [48,49]. Thus, direct contact with Sertoli cells in TOs + AT-MSCs may result in regulation of AT-MSCs proliferation and differentiation, mimicking the Sertoli cell and germ cell interaction in the testis. Peritubular myoid cells are located around the seminiferous tubules, contributing to the formation of the basement membrane along with Sertoli cells [50,51]. Peritubular myoid cells were identified using markers αSMA or COL1A. The αSMA protein is part of the cytoskeleton structure of peritubular myoid cells, modulating cell shape and contractility, while COL1A is a component of the basement membrane in which peritubular myoid cells adhere in the seminiferous tubule [52]. There are no reports of co-cultures of peritubular myoid cells with MSCs so far, so the potential interaction between both cell types have not been described. Based on our study, the expression of COL1A remained throughout the culture period in the TOs + AT-MSCs, whereas in the control TOs, the expression progressively decreased to nearly undetectable levels. Resulting proportions of peritubular myoid cells were higher in TOs + AT-MSCs compared to TOs. These results suggest that the presence of AT-MSCs influences the expression of COL1A; however, this effect should be further investigated in subsequent studies. Thus, increasing proportions of Leydig and peritubular myoid cells, and decreasing percentages of Sertoli cells in TOs + AT-MSCs, despite similar gene expression of mRNA of STAR, WT1 and αSMA , suggest that AT-MSCs induced a reorganization of tes-

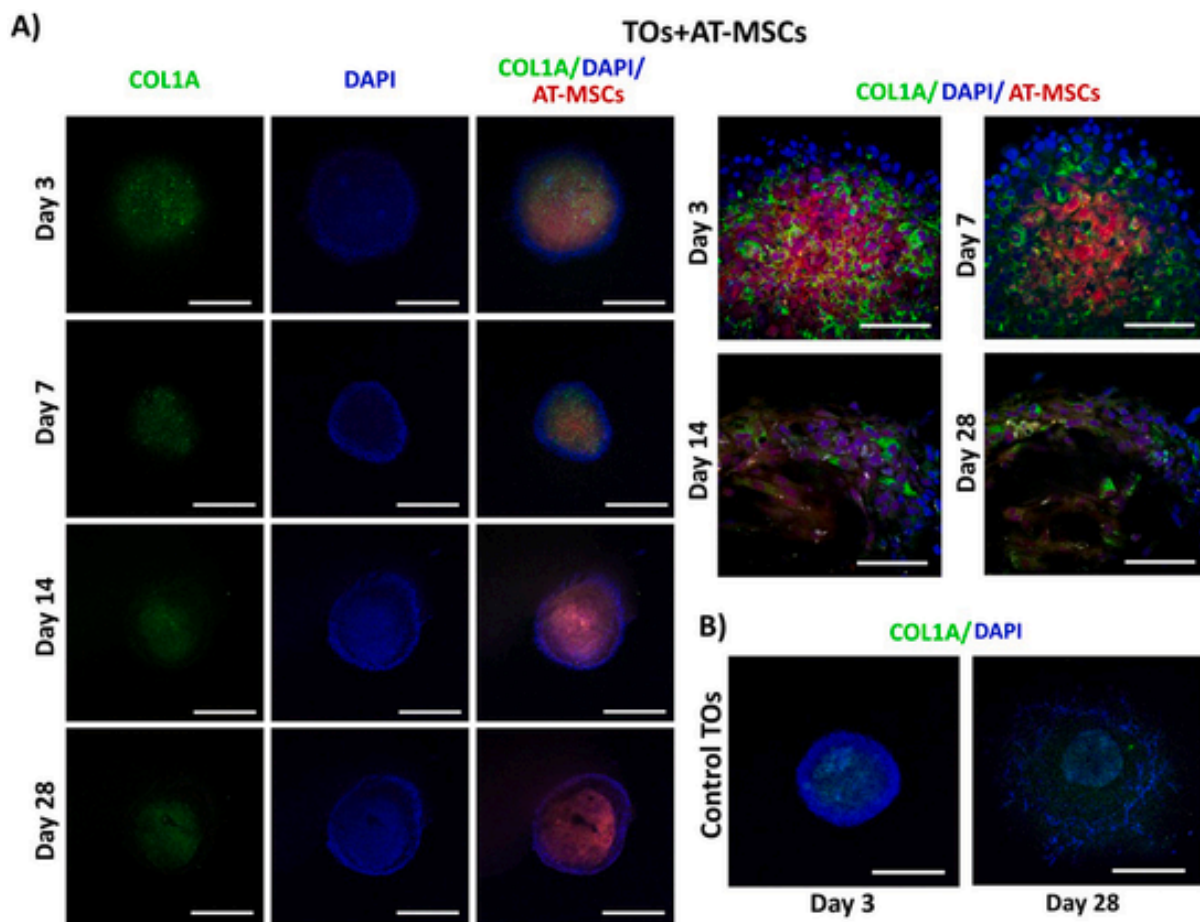


Fig. 7. Colocalization of Peritubular myoid cells and AT-MSCs in bovine TOs using confocal microscopy. (A) COL1A-positive cells in TOs + AT-MSCs are observed distributed within the central area throughout the culture period. (B) COL1A expression in control TOs at days 3 and 28 of culture. Cell nuclei were stained blue with DAPI. $n = 3$. Scale bars = 500 μm . (For interpretation of the references to colour in this figure legend, the reader is referred to the Web version of this article.)

ticular cells, changing the distribution and proportions of testicular cells.

Exposure to BMP4 has been shown to induce the expression of germ cell gene DAZL in MSCs in 2D cultures [53]. However, DAZL was not detected in AT-MSCs when co-cultured with testicular cells (TOs + AT-MSCs) or in control TOs. Previous 2D *in vitro* studies reported by our group indicated that a concentration of 100 ng/mL of BMP4 was sufficient to induce DAZL expression in MSCs induced to germ cell differentiation. However, due to the different properties of 3D TOs, it would be necessary to determine the optimal concentration of BMP4 in order to induce activation of DAZL in AT-MSCs. The lack of DAZL mRNA expression in TOs indicates that the isolation method used in testicular cells, allowed to eliminate the great majority of germ cells, which is one of the requirements to evaluate the potential germ cell differentiation of MSCs in this *in vitro* 3D model. However, the lack of DAZL expression in TOs + AT-MSCs also indicate that AT-MSCs did not express germ cell markers as a consequence of the absence of germ cell differentiation. FGF2 and GDNF are factors that are commonly used in the formation of TOs, as they promote the formation of structures similar to seminiferous cords and support the maintenance of germ cells [23,54]. These factors are produced by Sertoli cells and peritubular myoid cells which are important part of the testicular microenvironment and germ line development. On the other hand, it has been reported that FGF2 inhibits AT-MSC differentiation via the MAP kinase pathway and that it can promote proliferation of human AT-MSCs and stimulate cell cycle progression [55,56]. GDNF has similar effects on AT-MSCs, in addition to improving their anti-inflammatory capacity [57,58]. These, among other factors, constitute a fundamental aspect of *in vivo* testicular develop-

ment. Consequently, the composition of the culture medium is of paramount importance in fostering tubulogenesis and germ cell differentiation within the TO itself.

Several attempts have been made to isolate testicular cells from different species, with the goal of forming functional TOs [59,60]. Until now it has been possible to obtain TOs with structures similar to seminiferous tubules that have the capacity to produce testosterone and maintain germ cells, but the need for a functional TO model remained. The inclusion of AT-MSCs opened a new possibility for TO culture methods, by including cells that modulate and may improve testicular cell function and with the potential for germ cells differentiation.

5. Conclusion

Fetal bovine AT-MSCs can be co-cultured with Sertoli, Leydig and Peritubular myoid cells and can integrate, survive and modify the structure of the TOs, during a 28-day culture period. AT-MSCs induce the reorganization of testicular cells, particularly Leydig cells, thereby preventing the formation of branches and changing the distribution and proportions of testicular cells. The testicular microenvironment provided by TOs together with BMP4, FGF2 and GDNF is not sufficient to induce DAZL expression in AT-MSCs. The multifunctional reported properties of MSC, including their modulation of cell-cell interactions, ECM remodeling, angiogenic potential, anti-apoptotic effects, and regulation of cell migration, make them valuable candidates for enhancing functionality and stability of organoid systems.

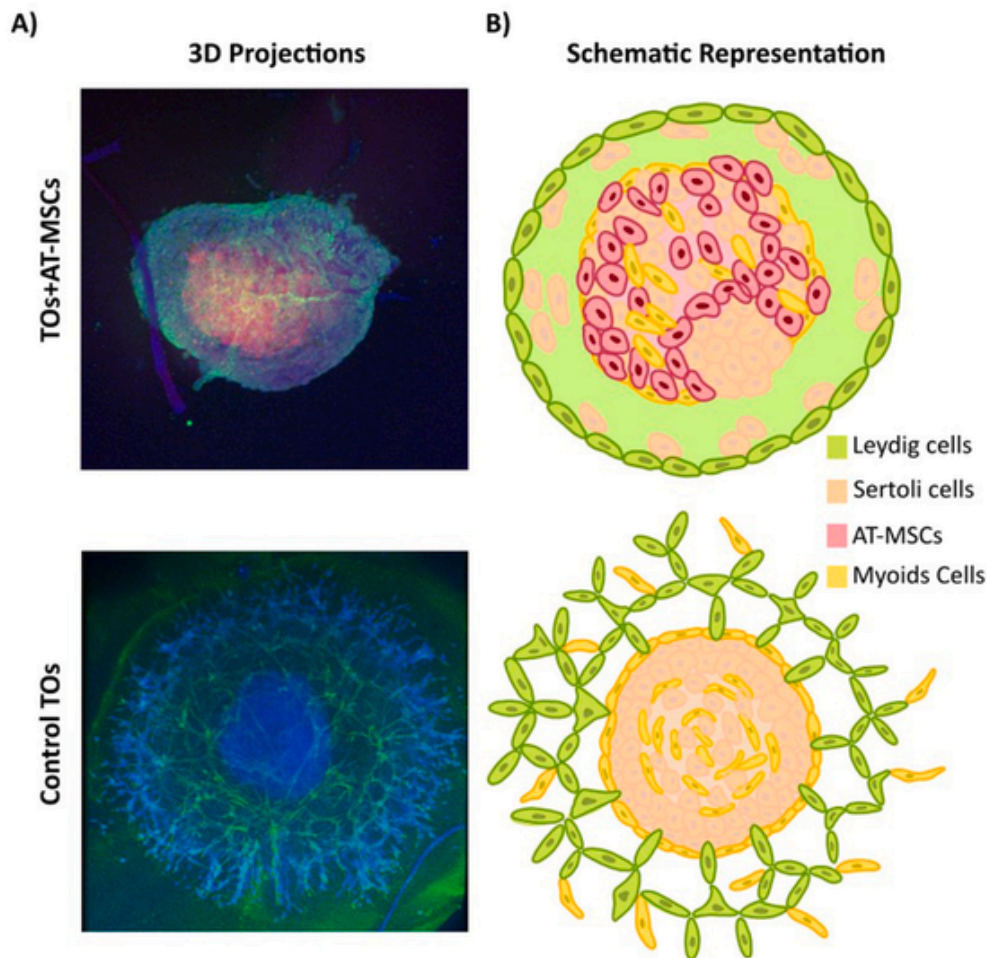


Fig. 8. Confocal microphotography and schematic representation of TOs + AT-MSCs and control TOs. (A) Projection of TOs + AT-MSCs and control TO at day 28 of culture. Co-culture of TOs + AT-MSCs composed of testicular cells and AT-MSCs. Leydig cells located in the outer area, while Sertoli cells, peritubular myoid cells, and AT-MSCs (PKH26; red) located in the central area. Bovine testicular cells forming control TOs present branching structures composed of Leydig and peritubular myoid cells. In the center of the structure, Sertoli cells were found along with peritubular myoid cells. (B) Schematic representation of the organization and localization of testicular cells and AT-MSCs in TOs + AT-MSCs and TOs. (For interpretation of the references to colour in this figure legend, the reader is referred to the Web version of this article.)

Funding

This study was supported by grants 1191114 and 1231145 from the National Research and Development Agency of Chile (ANID) from the Ministry of Education, Government of Chile.

Declaration of competing interest

None of the authors has any conflict of interest to declare.

CRediT authorship contribution statement

Jahaira Cortez: Conceptualization, Data curation, Formal analysis, Methodology, Validation, Visualization, Writing – original draft, Writing – review & editing. **Cristian G. Torres:** Conceptualization, Data curation, Formal analysis, Funding acquisition, Investigation, Project administration, Resources, Writing – original draft, Writing – review & editing. **Víctor H. Parraguez:** Conceptualization, Data curation, Formal analysis, Funding acquisition, Methodology, Resources, Writing – original draft, Writing – review & editing. **Mónica De los Reyes:** Data curation, Formal analysis, Investigation, Methodology, Writing – original draft, Writing – review & editing. **Oscar A. Peralta:** Conceptualization, Data curation, Formal analysis, Funding acquisition, Investiga-

tion, Methodology, Project administration, Resources, Software, Supervision, Validation, Visualization, Writing – original draft, Writing – review & editing.

References

- [1] Pittenger MF, Mbalaviele G, Black M, Mosca JD, Marshak DR. Mesenchymal Stem Cells. In: Koller, M.R., Palsson, B.O., Masters, J.R. (editors) Human Cell Culture. Human Cell Culture, vol vol. 5. Springer, Dordrecht. https://doi.org/10.1007/0-306-46870-0_9.
- [2] Wang C, Li Y, Yang M, Zou Y, Liu H, Liang Z, et al. Efficient differentiation of bone marrow mesenchymal stem cells into endothelial cells in vitro. *Eur J Vasc Endovasc Surg* 2018;55:257–65. <https://doi.org/10.1016/j.ejvs.2017.10.012>.
- [3] Leeman K.T, Pessina P, Lee J.H, Kim C.F. Mesenchymal stem cells increase alveolar differentiation in lung progenitor organoid cultures. *Sci Rep* 2019;9:6479. <https://doi.org/10.1038/s41598-019-42819-1>.
- [4] De Bari C, Dell'Accio F, Tylzanowski P, Luyten F.P. Multipotent mesenchymal stem cells from adult human synovial membrane. *Arthritis Rheum* 2001;44:1928–42. [https://doi.org/10.1002/1529-0131\(200108\)44:8<1928::AID-ART331>3.0.CO;2-P](https://doi.org/10.1002/1529-0131(200108)44:8<1928::AID-ART331>3.0.CO;2-P).
- [5] Stanko P, Kaiserova K, Altanerova V, Altaner C. Comparison of human mesenchymal stem cells derived from dental pulp, bone marrow, adipose tissue, and umbilical cord tissue by gene expression. *Biomed Pap Med Fac Univ Palacky Olomouc Czech Repub* 2014;158:373–7. <https://doi.org/10.5507/bp.2013.078>.
- [6] Asgari H.R, Akbari M, Abbasi M, Ai J, Korouji M, Aliakbari F, et al. Human Wharton's jelly-derived mesenchymal stem cells express oocyte developmental genes during co-culture with placental cells. *Iran J Basic Med Sci* 2015;18(1):22–9.
- [7] Aleahmad F, Ebrahimi S, Salmanezhad M, Azarnia M, Jaberipour M, Hoseini M, et al. Heparin/collagen 3D scaffold accelerates hepatocyte differentiation of

- wharton's jelly-derived mesenchymal stem cells. *Tissue Eng Regen Med* 2017;14:443–52. <https://doi.org/10.1007/s13770-017-0048-z>.
- [8] Zhang D, Liu X, Peng J, He D, Lin T, Zhu J, et al. Potential spermatogenesis recovery with bone marrow mesenchymal stem cells in an azoospermic rat model. *Int J Mol Sci* 2014;15:13151–65. <https://doi.org/10.3390/ijms150813151>.
- [9] Zheng S.X, Wang J, Wang X.L, Ali A, Wu L.M, Liu Y.S. Feasibility analysis of treating severe intrauterine adhesions by transplanting menstrual blood-derived stem cells. *Int J Mol Med* 2018;41:2201–12. <https://doi.org/10.3892/ijmm.2018.3415>.
- [10] Cho J, Kim T.H, Seok J, Jun J.H, Park H, Kweon M, et al. Vascular remodeling by placenta-derived mesenchymal stem cells restores ovarian function in ovariectomized rat model via the VEGF pathway. *Lab Invest* 2021;101:304–17. <https://doi.org/10.1038/s41374-020-00513-1>.
- [11] Karimghai N, Tamadon A, Rahmanifar F, Mehrabani D, Raayat Jahromi A, Zare S, et al. Spermatogenesis after transplantation of adipose tissue-derived mesenchymal stem cells in busulfan-induced azoospermic hamster. *Iran J Basic Med Sci* 2018;21:660–7. <https://doi.org/10.22038/IJBMS.2018.29040.7010>.
- [12] Kashani I.R, Zamani A.H, Soleimani M, Abdolvahabi M.A, Nayernia K, Shirazi R. Retinoic acid induces mouse bone marrow-derived CD15⁺, Oct4⁺ and CXCR4⁺ stem cells into male germ-like cells in a two-dimensional cell culture system. *Cell Biol Int* 2014;38:782–9. <https://doi.org/10.1002/cbin.10260>.
- [13] Ghasemzadeh-Hasankolaei M, Eslaminejad M.B, Batavani R, Ghasemzadeh-Hasankolaei M. Male and female rat bone marrow-derived mesenchymal stem cells are different in terms of the expression of germ cell specific genes. *Anat Sci Int* 2015;90:187–96. <https://doi.org/10.1007/s12565-014-0250-1>.
- [14] Segunda M.N, Díaz C, Torres C.G, Parraguez V.H, De Los Reyes M, Peralta O.A. Comparative analysis of the potential for germ cell (GC) differentiation of bovine peripheral blood derived-mesenchymal stem cells (PB-MSC) and spermatogonial stem cells (SSC) in Co-culture system with sertoli cells (SC). *Animals* 2023;13:318. <https://doi.org/10.3390/ani13020318>.
- [15] Oliver E, Alves-Lopes J.P, Harteveld F, Mitchell R.T, Åkesson E, Söder O, et al. Self-organising human gonads generated by a Matrigel-based gradient system. *BMC Biol* 2021;19:212. <https://doi.org/10.1186/s12915-021-01149-3>.
- [16] Yang Y, Huang R, Cao Z, Ma S, Chen D, Wang Z, et al. *In vitro* reconstitution of the hormone-responsive testicular organoids from murine primary testicular cells. *Biofabrication* 2022;15. <https://doi.org/10.1088/1758-5090/ac992a>.
- [17] Strange D.P, Zarandi N.P, Trivedi G, Atala A, Bishop C.E, Sadri-Ardekani H, et al. Human testicular organoid system as a novel tool to study Zika virus pathogenesis. *Emerg Microb Infect* 2018;7:82. <https://doi.org/10.1038/s41426-018-0080-7>.
- [18] Simian M, Bissell M.J. Organoids: a historical perspective of thinking in three dimensions. *J Cell Biol* 2017;216:31–40. <https://doi.org/10.1083/jcb.201610056>.
- [19] Fujii M, Matano M, Nanki K, Sato T. Efficient genetic engineering of human intestinal organoids using electroporation. *Nat Protoc* 2015;10:1474–85. <https://doi.org/10.1038/nprot.2015.088>.
- [20] Drost J, Karthaus W.R, Gao D, Driehuis E, Sawyers C.L, Chen Y, et al. Organoid culture systems for prostate epithelial and cancer tissue. *Nat Protoc* 2016;11:347–58. <https://doi.org/10.1038/nprot.2016.006>.
- [21] Takasato M, Er P.X, Chiu H.S, Little M.H. Generation of kidney organoids from human pluripotent stem cells. *Nat Protoc* 2016;11:1681–92. <https://doi.org/10.1038/nprot.2016.098>.
- [22] Baert Y, Dvorakova-Hortova K, Margaryan H, Goossens E. Mouse *in vitro* spermatogenesis on alginate-based 3D bioprinted scaffolds. *Biofabrication* 2019;11:035011. <https://doi.org/10.1088/1758-5090/ab1452>.
- [23] Alves-Lopes J.P, Söder O, Stukenborg J.B. Testicular organoid generation by a novel *in vitro* three-layer gradient system. *Biomaterials* 2017;130:76–89. <https://doi.org/10.1016/j.biomaterials.2017.03.025>.
- [24] Pendergraft S.S, Sadri-Ardekani H, Atala A, Bishop C.E. Three-dimensional testicular organoid: a novel tool for the study of human spermatogenesis and gonadotoxicity *in vitro*. *Biol Reprod* 2017;96:720–32. <https://doi.org/10.1095/biolreprod.116.143446>.
- [25] Sakib S, Uchida A, Valenzuela-Leon P, Yu Y, Valli-Pulaski H, Orwig K, et al. Formation of organotypic testicular organoids in microwell culture. *Biol Reprod* 2019;100:1648–60. <https://doi.org/10.1093/biolre/iox053>.
- [26] Cham T.C, Ibtisham F, Fayaz M.A, Honaramooz A. Generation of a highly biomimetic organoid, including vasculature, resembling the native immature testis tissue. *Cells* 2021;10:1696. <https://doi.org/10.3390/cells10071696>.
- [27] Cortez J, Leiva B, Torres C.G, Parraguez V.H, De Los Reyes M, Carrasco A, et al. Generation and characterization of bovine testicular organoids derived from primary somatic cell populations. *Animals* 2022;12:2283. <https://doi.org/10.3390/ani12172283>.
- [28] Gaur M, Ramathal C, Reijo Pera R.A, Turek P.J, John C.M. Isolation of human testicular cells and co-culture with embryonic stem cells. *Reproduction* 2018;155:153–66. <https://doi.org/10.1530/REP-17-0346>.
- [29] Kiani M, Movahedin M, Halvaei I, Soleimani M. Formation of organoid-like structures in the decellularized rat testis. *Iran J Basic Med Sci* 2021;24:1523–8. <https://doi.org/10.22038/IJBMS.2021.58294.12948>.
- [30] Sahu S, Albaugh M.E, Martin B.K, Patel N.L, Riffle L, Mackem S, et al. Growth factor dependency in mammary organoids regulates ductal morphogenesis during organ regeneration. *Sci Rep* 2022;12:7200. <https://doi.org/10.1038/s41598-022-11224-6>.
- [31] Richer G, Hobbs R.M, Loveland K.L, Goossens E, Baert Y. Long-term maintenance and meiotic entry of early germ cells in murine testicular organoids functionalized by 3D printed scaffolds and air-medium interface cultivation. *Front Physiol* 2021;12:757565. <https://doi.org/10.3389/fphys.2021.757565>.
- [32] Sakib S, Lara N.L.E.M, Huynh B.C, Dobrinski I. Organotypic rat testicular organoids for the study of testicular maturation and toxicology. *Front Endocrinol* 2022;13:892342. <https://doi.org/10.3389/fendo.2022.892342>.
- [33] Bresciani G, Holland L.J, Dogan F, Giamas G, Gagliano T, Zatelli M.C. Evaluation of spheroid 3D culture methods to study a pancreatic neuroendocrine neoplasm cell line. *Front Endocrinol* 2019;10:682. <https://doi.org/10.3389/fendo.2019.00682>.
- [34] Chanda D, Rehan M, Smith S.R, Dsouza K.G, Wang Y, Bernard K, et al. Mesenchymal stromal cell aging impairs the self-organizing capacity of lung alveolar epithelial stem cells. *Elife* 2021;10:e68049. <https://doi.org/10.7554/Elife.68049>.
- [35] Varzideh F, Pahlavan S, Ansari H, Halvaei M, Kostin S, Feiz M.S, et al. Human cardiomyocytes undergo enhanced maturation in embryonic stem cell-derived organoid transplants. *Biomaterials* 2019;192:537–50. <https://doi.org/10.1016/j.biomaterials.2018.11.033>.
- [36] Song L, Yuan X, Jones Z, Griffin K, Zhou Y, Ma T, et al. Assembly of human stem cell-derived cortical spheroids and vascular spheroids to model 3-D brain-like tissues. *Sci Rep* 2019;9:5977. <https://doi.org/10.1038/s41598-019-42439-9>.
- [37] Bourget J.M, Kérouédan O, Medina M, Rémy M, Thébaud N.B, Baille R, et al. Patterning of endothelial cells and mesenchymal stem cells by laser-assisted bioprinting to study cell migration. *BioMed Res Int* 2016;2016:3569843. <https://doi.org/10.1155/2016/3569843>.
- [38] Hung S.C, Pochampally R.R, Chen S.C, Hsu S.C, Prockop D.J. Angiogenic effects of human multipotent stromal cell conditioned medium activate the PI3K-Akt pathway in hypoxic endothelial cells to inhibit apoptosis, increase survival, and stimulate angiogenesis. *Stem Cell* 2007;25:2363–70. <https://doi.org/10.1634/stemcells.2006-0686>.
- [39] Bartosh T.J, Ylöstalo J.H, Mohammadipoor A, Bazhanov N, Coble K, Claypool K, et al. Aggregation of human mesenchymal stromal cells (MSCs) into 3D spheroids enhances their antiinflammatory properties. *Proc Natl Acad Sci U S A* 2010;107:13724–9. <https://doi.org/10.1073/pnas.1008117107>.
- [40] Zhang Z, Hill J, Holland M, Kurihara Y, Loveland K.L. Bovine sertoli cells colonize and form tubules in murine hosts following transplantation and grafting procedures. *J Androl* 2008;29:418–30. <https://doi.org/10.2164/jandrol.107.004465>.
- [41] Jiang Y, An X.L, Yu H, Cai N.N, Zhai Y.H, Li Q, et al. Transcriptome profile of bovine iPSCs derived from Sertoli Cells. *Theriogenology* 2020;146:120–32. <https://doi.org/10.1016/j.theriogenology.2019.11.022>.
- [42] Segunda M.N, Bahamonde J, Muñoz I, Sepulveda S, Cortez J, De Los Reyes M, et al. Sertoli cell-mediated differentiation of bovine fetal mesenchymal stem cells into germ cell lineage using an *in vitro* co-culture system. *Theriogenology* 2019;130:8–18. <https://doi.org/10.1016/j.theriogenology.2019.02.034>.
- [43] Bhushan S, Aslani F, Zhang Z, Sebastian T, Elsässer H.P, Klug J. Isolation of sertoli cells and peritubular cells from rat testes. *J Vis Exp* 2016;108:e53389. <https://doi.org/10.3791/53389>.
- [44] Luo L, Chen H, Zirkin B.R. Leydig cell aging: steroidogenic acute regulatory protein (StAR) and cholesterol side-chain cleavage enzyme. *J Androl* 2001;22:149–56. <https://doi.org/10.3390/ijms22042021>.
- [45] Galano M, Li Y, Li L, Sottas C, Papadopoulos V. Role of Constitutive STAR in Leydig Cells. *Int J Mol Sci* 2021;22:2021.
- [46] Chen F, Song L, Mauck R.L, Li W.J, Tuan R.S. *Mesenchymal stem cell*. In: Lanza R, Langer R, Vacanti J, editors. *Principles of tissue engineering*. third ed.; 2007. p. 823–43. New York: USA.
- [47] Wen Q, Wang Y, Tang J, Cheng C.Y, Liu Y.X. Sertoli cell Wt1 regulates peritubular myoid cell and fetal Leydig cell differentiation during fetal testis development. *PLoS One* 2016;11:e0167920. <https://doi.org/10.1371/journal.pone.0167920>.
- [48] Fan P, He L, Pu D, Lv X, Zhou W, Sun Y, et al. Testicular Sertoli cells influence the proliferation and immunogenicity of co-cultured endothelial cells. *Biochem Biophys Res Commun* 2011;404:829–33. <https://doi.org/10.1016/j.bbrc.2010.12.068>.
- [49] Zhang F, Hong Y, Liang W, Ren T, Jing S, Lin J. Co-culture with Sertoli cells promotes proliferation and migration of umbilical cord mesenchymal stem cells. *Biochem Biophys Res Commun* 2012;427:86–90. <https://doi.org/10.1016/j.bbrc.2012.09.007>.
- [50] Bernardino R.L, Alves M.G, Oliveira P.F. Establishment of primary culture of sertoli cells. *Methods Mol Biol* 2018;1748:1–8. https://doi.org/10.1007/978-1-4939-7698-0_1.
- [51] Crisóstomo L, Alves M.G, Gorga A, Sousa M, Riera M.F, Galardo M.N, et al. Molecular mechanisms and signaling pathways involved in the nutritional support of spermatogenesis by sertoli cells. *Methods Mol Biol* 2018;1748:129–55. https://doi.org/10.1007/978-1-4939-7698-0_11.
- [52] Jeanes A, Wilhelm D, Wilson M.J, Bowles J, McClive P.J, Sinclair A.H, et al. Evaluation of candidate markers for the peritubular myoid cell lineage in the developing mouse testis. *Reproduction* 2005;130:509–16. <https://doi.org/10.1530/rep.1.00718>.
- [53] Cortez J, Bahamonde J, De Los Reyes M, Palomino J, Torres C.G, Peralta O.A. *In vitro* differentiation of bovine bone marrow-derived mesenchymal stem cells into male germ cells by exposure to exogenous bioactive factors. *Reprod Domest Anim* 2018;53:700–9. <https://doi.org/10.1111/rda.13160>.
- [54] Vermeulen M, Del Vento F, Kanbar M, Pyr Dit Ruys S, Vertommen D, Poels J, et al. Generation of organized porcine testicular organoids in solubilized hydrogels from decellularized extracellular matrix. *Int J Mol Sci* 2019;20:5476. <https://doi.org/10.3390/ijms20215476>.
- [55] Lai W.T, Krishnappa V, Phinney D.G. Fibroblast growth factor 2 (Fgf2) inhibits differentiation of mesenchymal stem cells by inducing Twist2 and Spry4, blocking extracellular regulated kinase activation, and altering Fgf receptor expression levels. *Stem Cell* 2011;29:1102–11. <https://doi.org/10.1002/stem.661>.
- [56] Ma Y, Kakudo N, Morimoto N, Lai F, Taketani S, Kusumoto K. Fibroblast growth

- factor-2 stimulates proliferation of human adipose-derived stem cells via Src activation. *Stem Cell Res Ther* 2019;10:350. <https://doi.org/10.1186/s13287-019-1462-z>.
- [56] Wang Z, Li S, Wang Y, Zhang X, Chen L, Sun D. GDNF enhances the anti-inflammatory effect of human adipose-derived mesenchymal stem cell-based therapy in renal interstitial fibrosis. *Stem Cell Res* 2019;41:101605. <https://doi.org/10.1016/j.scr.2019.101605>.
- [57] Sun S, Zhang Q, Li M, Gao P, Huang K, Beejadhursing R, et al. GDNF promotes survival and therapeutic efficacy of human adipose-derived mesenchymal stem cells in a mouse model of Parkinson's disease. *Cell Transplant* 2020;29:963689720908512. <https://doi.org/10.1177/0963689720908512>.
- [58] Goldsmith T.M, Sakib S, Webster D, Carlson D.F, Van der Hoorn F, Dobrinski I. A reduction of primary cilia but not hedgehog signaling disrupts morphogenesis in testicular organoids. *Cell Tissue Res* 2020;380:191–200. <https://doi.org/10.1007/s00441-019-03121-8>.
- [59] Kanatsu-Shinohara M, Ogonuki N, Matoba S, Morimoto H, Shiromoto Y, Ogura A, et al. Regeneration of spermatogenesis by mouse germ cell transplantation into allogeneic and xenogeneic testis primordia or organoids. *Stem Cell Rep* 2022;17:924–35. <https://doi.org/10.1016/j.stemcr.2022.02.013>.
- [60] Pryzhkova M.V, Boers R, Jordan P.W. Modeling human gonad development in organoids. *Tissue Eng Regen Med* 2022;19:1185–206. <https://doi.org/10.1007/s13770-022-00492-y>.
- [61] Velasco V, Shariati S.A, Esfandyarpour R. Microtechnology-based methods for organoid models. *Microsyst Nanoeng* 2020;6:76. <https://doi.org/10.1038/s41378-020-00185-3>.
- [62] Alves-Lopes J.P, Söder O, Stukenborg J.B. Use of a three-layer gradient system of cells for rat testicular organoid generation. *Nat Protoc* 2018;13:248–59. <https://doi.org/10.1038/nprot.2017.140>.
- [63] Huaman O, Bahamonde J, Cahuascanco B, Jervis M, Palomino J, Torres C.G, et al. Immunomodulatory and immunogenic properties of mesenchymal stem cells derived from bovine fetal bone marrow and adipose tissue. *Res Vet Sci* 2019;124:212–22. <https://doi.org/10.1016/j.rvsc.2019.03.017>.
- [64] Cahuascanco B, Bahamonde J, Huaman O, Jervis M, Cortez J, Palomino J, et al. Bovine fetal mesenchymal stem cells exert antiproliferative effect against mastitis causing pathogen *Staphylococcus aureus*. *Vet Res* 2019;50:25. <https://doi.org/10.1186/s13567-019-0643-1>.
- [65] Jervis M, Huaman O, Cahuascanco B, Bahamonde J, Cortez J, Arias J.I, et al. Comparative analysis of in vitro proliferative, migratory and pro-angiogenic potentials of bovine fetal mesenchymal stem cells derived from bone marrow and adipose tissue. *Vet Res Commun* 2019;43:165–78. <https://doi.org/10.1007/s11259-019-09757-9>.